Research Square

Preprints are preliminary reports that have not undergone peer review.
They should not be considered conclusive, used to inform clinical practice,
or referenced by the media as validated information.

Dietary lemon alleviates hypercholesterolemia by elevating acetylcarnitine and activating CYP7A1-dependent bile acid synthesis

Yumei Zhang
National Key Laboratory of Agricultural Microbiology, Huazhong Agricultural University
Lei Cao
National Key Laboratory of Agricultural Microbiology, Huazhong Agricultural University
Xinxin Li
National Key Laboratory of Agricultural Microbiology, Huazhong Agricultural University
Li Zhou
National Key Laboratory of Agricultural Microbiology, Huazhong Agricultural University
Huansi Hu
National Key Laboratory of Agricultural Microbiology, Huazhong Agricultural University
Chuxing Cheng
National Key Laboratory of Agricultural Microbiology, Huazhong Agricultural University
Lingyu Jiang
National Key Laboratory of Agricultural Microbiology, Huazhong Agricultural University
Haiying Mao
National Key Laboratory of Agricultural Microbiology, Huazhong Agricultural University
Kun Huang
National Key Laboratory of Agricultural Microbiology, Huazhong Agricultural University
Ya Zhao
National Key Laboratory of Agricultural Microbiology, Huazhong Agricultural University
Xiaomei Sun
National Key Laboratory of Agricultural Microbiology, Huazhong Agricultural University
Xiaokun Liu
National Key Laboratory of Agricultural Microbiology, Huazhong Agricultural University
Qiang Zhang
National Key Laboratory of Agricultural Microbiology, Huazhong Agricultural University
Zhaocheng Ma
National Key Laboratory of Agricultural Microbiology, Huazhong Agricultural University
Zhong Zou
National Key Laboratory of Agricultural Microbiology, Huazhong Agricultural University

Meilin Jin

jinmeilin@mail.hzau.edu.cn

National Key Laboratory of Agricultural Microbiology, Huazhong Agricultural University

Article

Keywords: Hypercholesterolemia, Citrus limon, Acetylcarnitine, CYP7A1, Bile acid

Posted Date: November 11th, 2026

DOI: https://doi.org/10.21203/rs.3.rs-11029859/v1

License: This work is licensed under a Creative Commons Attribution 4.0 International License.
Read Full License

Additional Declarations: No competing interests reported.

Dietary lemon alleviates hypercholesterolemia by elevating acetylcarnitine and activating CYP7A1-dependent bile acid synthesis

Yumei Zhang[1,2], Lei Cao[1,2], Xinxin Li[1], Li Zhou[1], Huansi Hu[1], Chuxing Cheng[1,2], Lingyu Jiang[1,2], Haiying Mao[1,2], Kun Huang[1,3], Ya Zhao[1,3], Xiaomei Sun[1,4], Xiaokun Liu[1,3], Qiang Zhang[1,3], Zhaocheng Ma[1], Zhong Zou[1,4], Meilin Jin[1,2 *]

[1] National Key Laboratory of Agricultural Microbiology, Huazhong Agricultural University, Wuhan, People's Republic of China;

[2] Hubei Jiangxia Laboratory, Wuhan, People's Republic of China;

[3] Center for Frontier Crosses in Animal Diseases and One Health, Huazhong Agricultural University, Wuhan, People's Republic of China;

[4] College of Animal Medicine, Huazhong Agricultural University, Wuhan, People's Republic of China

[*]Corresponding author. Meilin Jin, No.1 Shizishan Street, Hongshan District, Wuhan, Hubei Province, China. E-mail: jinmeilin@mail.hzau.edu.cn.

Abstract

Lemon (*Citrus limon*) is a flavonoid-rich citrus fruit with potential lipid-lowering properties, but the mechanisms underlying these effects remain poorly understood. We evaluated lemon powder in mice fed a high-fat diet and investigated candidate mediators using metabolomics and hepatocyte experiments. Lemon powder reduced serum total cholesterol and low-density lipoprotein cholesterol, lowered hepatic cholesterol, and increased circulating acetylcarnitine and hepatic CRAT expression. Acetylcarnitine administration lowered cholesterol in mice with established diet-induced hypercholesterolemia and reduced lipid accumulation in fatty acid-treated HepG2 cells. Lemon powder increased hepatic cholesterol 7α-hydroxylase (CYP7A1) expression and fecal total bile acid levels; acetylcarnitine also increased hepatic CYP7A1. In HepG2 cells, CYP7A1 knockdown attenuated acetylcarnitine-induced cholesterol lowering. These findings identify acetylcarnitine as a candidate mediator of the response to lemon powder and support further evaluation of lemon-based dietary interventions.

Keywords: Hypercholesterolemia; *Citrus limon*; Acetylcarnitine; CYP7A1; Bile acid

Introduction

Elevated circulating cholesterol, particularly low-density lipoprotein cholesterol (LDL-C), is a major modifiable risk factor for atherosclerotic cardiovascular disease. Despite substantial geographical shifts in its distribution over recent decades, non-optimal cholesterol levels remain widespread worldwide [1]. Pharmacological therapies, including statins, cholesterol absorption inhibitors and proprotein convertase subtilisin/kexin type 9 (PCSK9) inhibitors, have markedly improved the clinical management of hypercholesterolemia [2,4]. However, adverse effects, variable treatment responses, poor long-term adherence and the high cost of some agents may limit their sustained or widespread use [3,4]. Dietary interventions that complement established therapies may therefore offer a practical approach to supporting long-term cholesterol control. Identifying food ingredients with reproducible lipid-lowering activity and defining their mechanisms of action are important steps towards developing such interventions.

Whole-body cholesterol homeostasis is maintained through the coordinated regulation of intestinal absorption, endogenous synthesis, tissue transport and elimination [5]. The liver has a central role in this process by converting cholesterol into bile acids, thereby providing a major route for cholesterol catabolism and disposal [6]. Cholesterol 7α-hydroxylase (CYP7A1) catalyses the first and rate-limiting reaction in the classical bile acid biosynthetic pathway [7]. The importance of this enzyme is illustrated by the hypercholesterolemic phenotype associated with CYP7A1 deficiency in humans and by the metabolic effects of hepatic Cyp7a1 overexpression in mice [8,9]. However, bile acid synthesis forms part of a broader enterohepatic system in which bile acid composition and signaling can also influence intestinal cholesterol absorption. For example, activation of the farnesoid X receptor (FXR) modifies bile acid metabolism and the intestinal handling of cholesterol [6]. Consequently, the effects of dietary ingredients on this system cannot be inferred from the expression of a single enzyme but require integrated assessment of molecular and metabolic responses.

Plant-derived foods contain structurally diverse bioactive compounds that may act on multiple components of lipid metabolism and have therefore attracted interest as

complementary dietary approaches to metabolic disorders [10]. Lemon (*Citrus limon*) is a widely consumed citrus fruit rich in flavonoids, organic acids and other phytochemicals, with reported antioxidant, anti-inflammatory, anti-obesity and antidiabetic activities [11-13]. Chromatographic studies of lemon juice have identified eriocitrin, hesperidin and other flavonoid glycosides, although their abundance varies among cultivars and grafting combinations [12,13]. Lemon-derived preparations have also shown metabolic activity in experimental models. Lemon peel polyphenols attenuated weight gain and altered the expression of lipid metabolism genes in mice fed a high-fat diet (HFD) [14], whereas a fermented lemon peel preparation improved several obesity-associated outcomes [15]. These observations support the potential use of lemon-derived ingredients in metabolic health.

Nevertheless, extracts, purified compounds and fermented preparations differ substantially from whole-fruit powder in chemical composition and bioavailability, and their biological effects cannot be directly extrapolated to the consumption of lemon powder. It remains unclear whether lemon powder improves cholesterol homeostasis during prolonged HFD feeding, which circulating metabolic changes accompany its consumption and whether these changes contribute to hepatic cholesterol regulation. Here, we characterized the chemical composition of lemon powder using liquid chromatography-high-resolution mass spectrometry (LC–HRMS) and evaluated its metabolic effects in a mouse model of HFD-induced hypercholesterolemia. Serum metabolomic profiling was subsequently used to identify candidate metabolites associated with lemon supplementation. Acetylcarnitine, which emerged from this analysis, was evaluated in separate treatment and prevention experiments and in fatty acid-treated HepG2 cells. Finally, CYP7A1 knockdown was used to determine whether this enzyme contributed to the cellular cholesterol response to acetylcarnitine. Through this integrated approach, we sought to characterize the cholesterol-lowering effects of lemon powder, identify a candidate circulating mediator and investigate its potential role in hepatic cholesterol catabolism, thereby providing a mechanistic basis for the development of lemon-derived dietary strategies for maintaining cholesterol

homeostasis.

Results

Chemical characterization and composition of lemon powder

Fresh lemons were sequentially sliced, freeze-dried, ground and sieved to obtain a homogeneous lemon powder (Fig. 1A). LC–HRMS analysis of the mixed reference standards showed distinct chromatographic peaks for citric acid, hesperetin and eriocitrin, with retention times of approximately 1.54, 18.31 and 24.52 min, respectively (Fig. 1B). In the lemon powder extract, peaks corresponding to eriocitrin and hesperetin were detected at retention times consistent with those of their respective reference standards, whereas no corresponding peak was observed for citric acid under the analytical conditions used (Fig. 1C). These results indicated the presence of eriocitrin and hesperetin in the lemon powder, while free citric acid was either absent or present below the detection limit.

Untargeted chemical profiling further revealed the compositional complexity of the lemon powder, 1247 unique differential small molecules were identified in the lemon, which were further categorized into 9 classes of compounds. Among these, flavonoids were the most abundant, accounting for 410 small molecules (Figure 1D) and representing 32.88% of all identified compounds. Collectively, these findings demonstrated that the lemon powder contained a chemically diverse phytochemical profile dominated by flavonoid constituents.

Lemon supplementation alleviates diet-induced hypercholesterolemia

An initial 28-day study examined lemon powder at 50-400 mg/kg in mice fed a normal diet (Figure S1A). Lemon supplementation significantly reduced body weight gain (Figure S1B) without affecting daily food intake (Figure S1C). Serum biochemical analysis further showed reduced levels of LDL-C and aspartate aminotransferase (AST) levels (Figure S1D and E). At 200 mg/kg, lemon treatment upregulated hepatic expression of cholesterol metabolism-related genes, including farnesoid X receptor (FXR), cytochrome P450 7A1 (CYP7A1), and 12α-hydroxylase (CYP8B1), while downregulating small heterodimer partner (SHP) and oxysterol 7α-hydroxylase

(CYP7B1) (Figure S1F). This dose produced the clearest lipid-related response without increasing serum AST and was selected for the long-term study.

We next evaluated lemon powder in mice with HFD-induced hypercholesterolemia. Eight-week-old male C57BL/6J mice were fed a normal diet (ND, 3.85 kcal/g), HFD (5.22 kcal/g), or HFD supplemented with 200 mg/kg lemon powder (HFDL, 5.22 kcal/g) for seven months (Figure 2A). Compared with HFD controls, HFDL mice gained less body weight after day 120 (Figure 2B), despite similar energy intake and water consumption (Figure S2A and B). Liver, inguinal white adipose tissue (iWAT), and interscapular brown adipose tissue (iBAT) indices were also lower in HFDL mice (Figure 2C and D). Moreover, lemon supplementation significantly reduced serum total cholesterol and LDL-C levels throughout the experimental period (Figure 2E). Hepatic cholesterol quantification and histological analyses further confirmed reduced lipid accumulation in HFDL mice (Figure 2F and G). Collectively, these results demonstrate that lemon supplementation effectively ameliorates HFD-induced hypercholesterolemia.

Lemon supplementation reshapes host metabolism and elevates acetylcarnitine

To identify the metabolic changes underlying the cholesterol-lowering effects of lemon, untargeted serum metabolomics was performed in ND, HFD, and HFDL mice. Partial least squares discriminant analysis (PLS-DA) revealed clear separation among the three dietary groups (Figure 3A), indicating substantial metabolic remodeling induced by lemon supplementation. Variable importance in projection (VIP) analysis further identified a set of metabolites significantly altered in HFDL mice relative to HFD controls (Figure 3B), many of which showed marked abundance differences across groups (Figure 3C). Among these metabolites, acetylcarnitine and arginine were the most prominently increased in HFDL mice, with acetylcarnitine displaying markedly higher abundance compared with arginine (Figure 3D). Correlation analysis further revealed a significant negative association between serum acetylcarnitine levels and total cholesterol concentrations (Figure 3E), suggesting a potential role of acetylcarnitine in mediating the lipid-lowering effects of lemon. We next examined

whether lemon supplementation could influence acetylcarnitine biosynthesis. Expression of carnitine acetyltransferase (CRAT), a key enzyme responsible for acetylcarnitine production, was significantly upregulated in HFDL mice compared with HFD controls (Figure 3F), indicating lemon supplementation enhanced host capacity for acetylcarnitine synthesis.

Acetylcarnitine alleviates hypercholesterolemia *in vivo* and *in vitro*

To determine whether acetylcarnitine directly contributes to cholesterol reduction, we evaluated its metabolic effects in an HFD-induced hypercholesterolemia mouse model (Figure 4A). Administration of acetylcarnitine significantly reduced serum total cholesterol and LDL-C levels compared with HFD controls (Figure 4B and C). Histological staining further revealed that acetylcarnitine treatment markedly alleviated hepatic lipid accumulation induced by HFD feeding (Figure 4D), accompanied by a significant reduction in hepatic total cholesterol levels (Figure 4E). Importantly, serum ALT and AST levels were not altered by acetylcarnitine treatment (Figure 4F), indicating good tolerability at the administered dose. Consistent with these results, pharmacokinetic analysis demonstrated a significant increase in hepatic acetylcarnitine concentrations in treated mice (Figure 4G), confirming effective systemic absorption and liver accumulation.

A preventive experiment further demonstrated that co-administration of acetylcarnitine with HFD for two months significantly attenuated diet-induced increases in serum cholesterol levels (Figure S3), supporting a protective role for acetylcarnitine in hypercholesterolemia.

To further examine its cellular effects, *in vitro* experiments were performed using HepG2 cells. Treatment with 50 μM acetylcarnitine did not affect cell viability (Figure S4A). Under lipotoxic conditions induced by sodium oleate and sodium palmitate, acetylcarnitine significantly reduced intracellular triglyceride and total cholesterol levels (Figure 4H). Consistently, filipin staining confirmed that acetylcarnitine markedly suppressed intracellular accumulation of unesterified cholesterol (Figure 4I). Together, these results demonstrate that acetylcarnitine exerts cholesterol-lowering

effects both *in vivo* and *in vitro*.

Acetylcarnitine promotes CYP7A1-dependent bile acid synthesis

We next investigated the molecular mechanism underlying this effect. Analysis of cholesterol metabolism-related genes (Figure 5A) revealed that lemon supplementation significantly upregulated both mRNA and protein levels of CYP7A1, key enzymes in the classical bile acid synthesis pathway (Figure 5B and C). Consistently, bile acid profiling showed substantial remodeling of fecal bile acid composition in HFDL mice, including reduced levels of hyodeoxycholic acid (HDCA), taurocholic acid 3-sulfate (TCA-3S), β-hyodeoxycholic acid (3β-HDCA), 5-β-cholanic acid-3α-ol-6-one (6-ketoLCA), tauro-ω-muricholic acid (Tω-MCA), tauro-β-muricholic acid (Tβ-MCA), lithocholic acid (LCA), and taurocholic acid (TCA), while cholic acid 7-sulfate (CA-7S) was significantly increased (Figure S5). Notably, total fecal bile acids excretion was markedly elevated in HFDL mice compared with HFD controls (Figure 5D), indicating lemon enhanced cholesterol catabolism through bile acid synthesis.

Importantly, acetylcarnitine treatment also significantly increased CYP7A1 expression in mouse liver (Figure 6A), as demonstrated by immunofluorescence staining and western blot analysis (Figure 6B and C). Consistent results were obtained in HepG2 cells, where acetylcarnitine treatment markedly upregulated CYP7A1 protein levels (Figure 6D). To verify whether CYP7A1 mediates acetylcarnitine-induced cholesterol reduction, we performed gene knockdown experiments. Among two CYP7A1-specific siRNAs tested in 293T and HepG2 cells, siCYP7A1-2 showed the highest knockdown efficiency and was selected for subsequent experiments (Figure 6E and Figure S4B). Silencing CYP7A1 largely abolished the ability of acetylcarnitine to reduce intracellular cholesterol levels and attenuated the induction of CYP7A1 expression (Figure 6F), demonstrating that CYP7A1 is essential for acetylcarnitine-mediated cholesterol regulation. Taken together, these findings indicate that acetylcarnitine alleviates hypercholesterolemia primarily by stimulating the classical bile acid synthesis pathway through CYP7A1 upregulation.

Discussion

In the present study, dietary lemon powder supplementation attenuated hypercholesterolemia induced by prolonged high-fat diet (HFD) feeding in mice. By integrating chemical profiling, serum metabolomics and functional experiments, we identified acetylcarnitine as a candidate mediator linking lemon consumption to cholesterol homeostasis. Lemon supplementation increased circulating acetylcarnitine concentrations and hepatic expression of carnitine acetyltransferase (CRAT), the enzyme that catalysis the reversible formation of acetylcarnitine from acetyl-CoA and carnitine. In complementary intervention experiments, acetylcarnitine reduced circulating and cellular cholesterol accumulation and increased CYP7A1 expression, whereas CYP7A1 silencing markedly attenuated its cholesterol-lowering effect in hepatocytes. Collectively, these findings suggest that lemon improves cholesterol homeostasis through an acetylcarnitine-CYP7A1-bile acid axis, providing mechanistic insight into the metabolic benefits of dietary phytochemicals in hypercholesterolemia.

Chemical profiling showed that flavonoids were the largest class of compounds annotated in the lemon powder. Eriocitrin was confirmed by comparison with a reference standard, consistent with previous analyses identifying this flavanone glycoside as a characteristic constituent of lemon peel [16,17]. By contrast, citric acid was not detected under the analytical conditions used. Given the established occurrence of citric acid in lemon, this observation should not be interpreted as evidence of its complete absence. Matrix-dependent ion suppression, extraction selectivity or a concentration below the detection limit may have contributed to the lack of a corresponding chromatographic peak. Targeted quantitative analysis using a validated method is therefore required to clarify its abundance.

The cholesterol-lowering phenotype observed here is consistent with previous evidence that lemon-derived preparations and citrus flavonoids can modulate lipid metabolism [11,15,18-20]. Lemon peel and other citrus fractions contain complex mixtures of flavanone glycosides, phenolic acids, dietary fiber and other phytochemicals that may act through complementary mechanisms[11]. In cholesterol-fed *Ldlr*$^{-/-}$ mice, the citrus flavanone naringenin ameliorated hyperlipidemia and hepatic steatosis by

enhancing hepatic fatty acid oxidation and suppressing fatty acid synthesis, while also attenuating hepatic and systemic inflammation [21]. Eriocitrin, a characteristic lemon flavonoid, has similarly been shown to alleviate diet-induced hepatic steatosis in mice, accompanied by enhanced mitochondrial biogenesis and fatty acid oxidation [22]. Hesperidin also improved hyperlipidemia and hepatic steatosis in HFD-fed *Ldlr*$^{-/-}$ mice and modulated proteins involved in lipid synthesis and reverse cholesterol transport, including ACCα, FAS, ABCG8, ABCA1 and ABCG1[23]. Moreover, α-glucosyl hesperidin and water-dispersible hesperetin reduced plasma total cholesterol, atherosclerotic plaque formation and macrophage infiltration in apolipoprotein E-deficient mice [24]. Collectively, these studies indicate that citrus flavonoids can influence multiple components of lipid homeostasis, including hepatic lipid synthesis, mitochondrial fatty acid oxidation, cholesterol transport and inflammation. However, these effects depend on compound structure, dose, formulation and bioavailability, and findings obtained with purified flavonoids or concentrated preparations cannot be directly extrapolated to whole lemon powder.

Acetylcarnitine links mitochondrial acetyl-CoA handling with cellular energy metabolism [25]. Carnitine acetyltransferase buffers the mitochondrial acetyl-CoA pool through reversible formation of acetylcarnitine and can thereby influence metabolic flexibility [26,27]. Lemon supplementation increased serum acetylcarnitine and hepatic CRAT expression, suggesting that the host response, rather than direct transfer of acetylcarnitine from the powder, contributed to the circulating metabolite signal. The upstream pathway through which lemon constituents induce CRAT remains unknown. Functionally, acetylcarnitine exhibited significant cholesterol-lowering activity in both *in vivo* and *in vitro* experiments. Administration of acetylcarnitine reduced serum total cholesterol and LDL-C levels in HFD-fed mice and alleviated hepatic lipid accumulation, consistent with its known role in regulating lipid metabolism. Mechanistically, our data demonstrate that acetylcarnitine promotes cholesterol catabolism through activation of the classical bile acid synthesis pathway. Specifically, acetylcarnitine markedly upregulated the expression of CYP7A1, the rate-limiting

enzyme responsible for converting cholesterol into bile acids [28-30]. The CYP7A1-mediated pathway represents the primary route for hepatic cholesterol elimination [31]. Consistent with this mechanism, lemon supplementation significantly increased fecal bile acid excretion, indicating enhanced conversion of cholesterol into bile acids and subsequent elimination from the body. Importantly, silencing CYP7A1 largely abolished the cholesterol-lowering effects of acetylcarnitine in hepatocytes, confirming that CYP7A1 is essential for acetylcarnitine-mediated regulation of cholesterol metabolism.

Several limitations of the present study should be noted. First, while acetylcarnitine was identified as a key metabolite contributing to cholesterol reduction and hepatic CRAT upregulation was observed, the specific bioactive components in lemon responsible for driving this metabolic remodeling, as well as the upstream mechanisms underlying hepatic CRAT induction, remain to be fully defined. Citrus fruits contain diverse flavonoids, including eriocitrin, hesperidin, and neohesperidin, which may contribute to these effects. Second, whether additional pathways beyond CYP7A1-mediated bile acid synthesis contribute to the cholesterol-lowering effect of acetylcarnitine warrants further investigation. Future studies combining metabolite tracing, hepatocyte models, and targeted knockdown approaches will be required to further elucidate the complete molecular pathways involved in this process.

In conclusion, this study reveals that lemon alleviates hypercholesterolemia by elevating acetylcarnitine, which activates hepatic CYP7A1-mediated bile acid synthesis and cholesterol catabolism. These findings identify an acetylcarnitine-CYP7A1 axis as a mechanism underlying the cholesterol-lowering effect of lemon, expanding our understanding of dietary phytochemical regulation of host lipid metabolism and supporting the development of lemon-derived phytotherapeutic strategies for hypercholesterolemia management.

Methods

Preparation of lemon powder

Fresh lemons (*Citrus limon*) were purchased from Anyue County, Sichuan

Province, China. The fruits were cut into slices and freeze-dried at −35 °C for 48 h. The dried slices were ground and passed through a 100-mesh sieve to obtain lemon powder.

LC–HRMS analysis of lemon powder

Reference standards of citric acid, hesperetin and eriocitrin (Shanghai Yuanye Bio-Tech Co., Ltd., B21313, B20184, and B21159) were dissolved in 80% (v/v) methanol and combined to give a mixed solution containing 100 μg mL^{-1} of each compound. The solution was filtered through a 0.22 μm membrane. For sample extraction, approximately 8.1 mg of lemon powder was extracted with 1 mL of 80% (v/v) methanol and ultrasonically extracted for 10 min. After standing, the supernatant was collected and filtered through a 0.22-μm membrane filter before instrumental analysis.

Analysis was performed using a Dionex UltiMate 3000 ultrahigh-performance liquid chromatography system coupled to a Q Exactive Orbitrap high-resolution mass spectrometer (Thermo Scientific). Separation was performed on a Welchrom Ultimate LP-C18 column (100 × 2.1 mm, 1.8 μm) at 47 °C. Mobile phase A was ultrapure water containing 0.1% (v/v) formic acid and 5 mM ammonium formate; mobile phase B was acetonitrile. The flow rate was 0.30 mL min^{-1}, and the injection volume was 10.0 μL. The gradient was 3% B at 0–3 min, 6% B at 4–5 min, 10% B at 6–10 min, 13% B at 14 min, 15% B at 17 min, 20% B at 19 min, 25% B at 21 min, 30% B at 22 min, 80% B at 23–26 min and 3% B at 27–30 min.

The mass spectrometer used a heated electrospray ionization source in positive- and negative-ion modes. Sheath and auxiliary gas flow rates were 40 and 10 arbitrary units, respectively. Spray voltage magnitudes were 3.8 kV in positive-ion mode and 3.0 kV in negative-ion mode. The capillary temperature was 320 °C, the auxiliary gas heater temperature was 350 °C, and the S-lens RF level was 50. Data were acquired in full-scan/data-dependent MS/MS Top10 mode. Full-scan spectra were acquired over *m/z* 100–1200 at a resolving power of 70,000, and MS/MS spectra were acquired from *m/z* 50 at a resolving power of 17,500. Higher-energy collisional dissociation used

stepped normalized collision energies of 15, 30 and 45.

Extracted-ion chromatograms were generated from the positive- and negative-ion datasets using a mass tolerance of 10 ppm. The monitored protonated and deprotonated ions were *m/z* 193.03428 and 191.01973 for citric acid, *m/z* 303.08631 and 301.07176 for hesperetin, and *m/z* 597.18140 and 595.16684 for eriocitrin, respectively. The corresponding full-scan and tandem mass spectra were retrieved according to the retention times of the extracted chromatographic peaks.

UHPLC–ESI–QTRAP–MS/MS analysis of lemon powder

Approximately 50 mg of sample powder was extracted with 1.2 mL of 70% (v/v) methanol containing the internal standard. The mixture was vortexed for 30 s at 30-min intervals for a total of six cycles and subsequently centrifuged at 12,000 rpm for 10 min at 4 °C. The resulting supernatant was passed through a 0.22-μm microporous membrane filter and transferred into an autosampler vial for UHPLC–ESI–QTRAP–MS/MS analysis.

Chromatographic separation was performed using a Nexera X2 UHPLC system (Shimadzu, Kyoto, Japan) equipped with an Agilent SB-C18 column (100 mm × 2.1 mm, 1.8 μm; Agilent Technologies, Santa Clara, CA, USA). The mobile phases consisted of water containing 0.1% (v/v) formic acid (mobile phase A) and acetonitrile containing 0.1% (v/v) formic acid (mobile phase B). The gradient was initiated at 5% B, increased linearly to 95% B over 9 min and maintained at 95% B for 1 min. The proportion of mobile phase B was then returned to 5% within 1.1 min, followed by re-equilibration at the initial conditions for 2.9 min. The flow rate was maintained at 0.35 mL min−1, the column temperature was set to 40 °C, and the injection volume was 4 μL. The column effluent was introduced into a 4500 QTRAP triple-quadrupole linear ion-trap mass spectrometer (SCIEX, Framingham, MA, USA) equipped with an electrospray ionisation source.

The electrospray ionisation source was operated at 550 °C with ion-spray voltages of 5.5 kV in positive-ion mode and −4.5 kV in negative-ion mode. Ion-source gases 1 and 2 and the curtain gas were maintained at 50, 60 and 25 psi, respectively. The

collision-activated dissociation setting was set to high. Instrument tuning and mass calibration were performed using polypropylene glycol solutions at 10 and 100 μmol L−1 in triple-quadrupole and linear ion-trap modes, respectively. Data were acquired in multiple-reaction monitoring mode using nitrogen as the collision gas at the medium setting. The declustering potential and collision energy were individually optimised for each multiple-reaction monitoring transition. Scheduled sets of transitions were monitored according to the chromatographic elution windows of the corresponding metabolites.

Animal experiments

Specific pathogen-free (SPF) C57BL/6J male mice were obtained from the Laboratory Animal Center of Huazhong Agricultural University (Wuhan, China; Certificate No.: SCXK (e) 2020-0084) and housed under SPF conditions (12 h light/dark cycle, 22 ± 2 °C, 45 ± 5% relative humidity) with ad libitum access to water and food. The normal chow diet (ND) contained 10% fat, 20% protein, and 70% carbohydrate, while the high-fat diet (HFD) contained 60% fat, 15% protein, and 25% carbohydrate. All animal procedures were performed in accordance with the Guide for the Laboratory Animal Ethics Committee of Huazhong Agricultural University, Wuhan, China (No. HZAUMO-2022-0096).

For the short-term dose-screening experiment, 8-week-old C57BL/6J male mice were acclimated for one week on a chow diet ad libitum and randomly assigned into five groups (n=5 per group): the control (Ctrl) and Ctrl supplemented with 50, 100, 200, or 400 mg/kg of lemon powder, respectively. The intervention lasted for 28 days.

For long-term lemon intervention experiment, mice were acclimated as above and divided into three groups (n=12 per group): the normal chow diet group (ND), the high-fat diet group (HFD) and the HFD with 200 mg/kg lemon powder group (HFDL). The intervention lasted for 210 days.

For acetylcarnitine treatment study, 8-week-old C57BL/6J male mice were fed with normal chow diet (ND, n=8) or HFD (n=16) for 12 months. After which, the HFD mice were subdivided into two groups (n=8 per group): the HFD group and the HFD

with 50 mg/kg acetylcarnitine (HFDA, oral gavage; MCE, NJ, USA, #HY-126358) group. And the interventions were lasted for another one month.

For acetylcarnitine prevention study, 8-week-old mice were fed a control chow diet ad libitum for one week and then randomly divided into three groups (n=6 per group): control group receiving a normal chow diet (ND), HFD group, and HFD oral gavage with 50 mg/kg acetylcarnitine (HFDA). The interventions were continued for two months.

Serum biochemical index and hepatic total cholesterol measurements

Serum alanine aminotransferase (ALT), aspartate aminotransferase (AST), total cholesterol, triglyceride, high-density lipoprotein cholesterol (HDL-C), and LDL-C were measured using an Automated Biochemistry Analyzer (BS-190, Mindray, Shenzhen, China). Hepatic total cholesterol levels were measured using the commercial kits (Applygen, Beijing, China) following the manufacturer's instructions.

Hematoxylin-eosin (H&E) and Oil Red O (ORO) staining

For H&E staining, liver tissues were fixed with 4% paraformaldehyde and embedded in paraffin. Sections of 5 μm thickness were blocked and deparaffinized with xylene followed standard H&E protocols.

For ORO staining, liver tissues were fixed with 4% paraformaldehyde and incubated in ORO solution for 8~10 minutes. Next, differentiation was carried out using 60% isopropanol, followed by counterstaining with hematoxylin for 3~5 minutes in accordance with established protocols.

Immunofluorescence staining

Paraffin-embedded liver sections were retrieved using a 0.01 M citrate buffer solution, and blocked with 5% bovine serum albumin (BSA; Sigma-Aldrich), followed by staining with anti-CYP7A1 primary antibody (Proteintech, 1:500) and incubated with the goat anti-rabbit CY3 conjugated secondary antibody (Abcam, Cambridge, UK). Images were captured using an orthogonal fluorescence microscope (Nikon, Tokyo, Japan).

Quantitative real-time PCR (qRT-PCR)

Liver RNA was extracted, reverse transcribed, and analyzed using ABI QuantStudio 6 (Applied Biosystems). The primers (Supplementary Table 1) were designed and synthesized by Sango Biotech (Wuhan) Co., Lt. The relative expression levels of target genes were calculated by comparing ($_{\Delta\Delta}$Ct) with β-actin.

Western blot analysis

Total proteins extracted from liver tissues or cultured cells were separated by SDS-PAGE and transferred onto PVDF membranes. The membranes were incubated with primary antibodies against CYP7A1 (Proteintech, #18054-1-AP) and GAPDH (Proteintech, #60004-1-Ig), followed by incubation with appropriate secondary antibodies. GAPDH was used as an internal loading control. Protein signals were visualized using an enhanced chemiluminescence (ECL) detection system (Tanon, Beijing, China).

Fecal bile acids analysis

For fecal bile acid extraction, 20 mg of fecal samples were homogenized using a ball mill and subsequently extracted with 500 μL of methanol. To ensure accurate quantification, 10 μL of an internal standard (IS) mixed solution (1 μg/mL) was added to each sample. The mixtures were incubated at -20 °C for 10 min to precipitate proteins, followed by centrifugation at 12000 × g for 10 min at 4 °C. The supernatants were collected, evaporated to dryness under nitrogen, and reconstituted for liquid chromatography-tandem mass spectrometry (LC-MS/MS) analysis. LC-MS/MS analysis was performed using the 6500 QTRAP system (Applied Biosystems) equipped with an electrospray ionization (ESI) source. Chromatographic separation was achieved using a Waters ACQUITY UPLC HSS T3 C18 column (100 mm × 2.1 mm, 1.8 μm particle size). The mobile phase consisted of (A) 5 mM ammonium acetate in water with 0.01% acetic acid and (B) acetonitrile with 0.01% acetic acid. The gradient elution program was as follows: 5–40% B over 0.5 min, 40–50% B over 4 min, 50–75% B over 3 min, 75–95% B over 2.5 min, 95% B for 2 min, and re-equilibration at 5% B for 2 min (total run time: 14 min). The analysis was performed with a flow rate of 0.35 mL/min, column temperature of 40 °C, and injection volume of 1 μL. Bile acids were

quantified using scheduled multiple reaction monitoring (MRM) in negative ion mode. Data acquisition and processing conducted using Analyst 1.6.3 and Multiquant 3.0.3 software (Sciex), respectively.

Serum untargeted metabolomics profiling

Metabolite profiling of fasting blood samples was analyzed using ultra-high-performance liquid chromatography (UHPLC; 1290 Infinity LC, Agilent Technologies) -QTOF MS (AB Sciex TripleTOF 6600) (Shanghai Applied Protein Technology Co., Ltd). For metabolite extraction, samples were homogenized in 1000 μL of methanol/acetonitrile/water (2:2:1, v/v/v) and centrifuged at 14000 × g for 15 min at 4 °C. The supernatant was dried using a vacuum centrifuge and reconstituted in 100 μL of acetonitrile/water (1:1, v/v). Chromatographic separation employed a Waters ACQUITY UPLC BEH column (2.1 × 100 mm, 1.7 μm) with a mobile phase: (A) water containing 25 mM ammonium acetate/ammonium hydroxide and (B) acetonitrile. The gradient elution program included: 85% B for 1 min, linearly reduced to 65% B over 11 min, decreased to 40% B in 0.1 min and held for 4 min, then increased to 85% B in 0.1 min, followed by a 5 min re-equilibration period.

Mass spectrometry analysis used dual electrospray ionization (ESI) modes with parameters: Ion Source Gas1 (Gas1)/(Gas2) at 60 psi, curtain gas (CUR) at 30 psi, 600 °C source temperature, and IonSpray Voltage Floating (ISVF) at ± 5500 V. For MS acquisition, the mass range was set to m/z 60–1000 Da with an accumulation time of 0.20 s/spectra. Auto MS/MS acquisition was performed over a mass range of m/z 25–1000 Da with an accumulation time of 0.05 s/spectra. Information-dependent acquisition (IDA) was used for product ion scanning in high-sensitivity mode, with the following settings: collision energy (CE) fixed at 35 V (±15 eV), declustering potential (DP) ± 60 V, isotope exclusion 4 Da, and 10 candidate ions per cycle monitoring. Data processing involved conversion to MzXML (ProteoWizard) followed by XCMS analysis.

Targeted metabolomics profiling of acetylcarnitine

Weighted liver tissues were extracted with 500 μL cold methanol: water (3:1, v/v,

-20 °C), vortexed for 30 s, incubated at -20 °C for 1 h followed by centrifuging with12000 rpm at 4 °C for15 min. Supernatants were collected undiluted (culture medium) or 100-fold diluted (10 μL liver extract) for LC-MS/MS analysis.

Working standards were prepared by diluting 100 μL stock solutions to 10 mL, followed by serial dilution for calibration curves. Chromatographic separation was performed on a Waters ACQUITY UPLC system with BEH Amide column (2.1 × 100 mm, 1.7 μm) using 0.1% formic acid (A) and acetonitrile (B) at 300 μL/min (40 °C column, 10 °C autosampler, 1 μL injection). Mass spectrometry was performed using a Waters Xevo TQ-XS spectrometer equipped with an electrospray ionization (ESI) interface under optimized parameters: capillary voltage -2500 V, cone 30 V, desolvation 550 °C (1000 L/h), collision gas 0.15 mL/min, and nebulizer 7 bar. Multiple reaction monitoring (MRM) transitions were established via standard infusion, selecting the most sensitive Q1/Q3 pair for quantification with secondary transitions for confirmation. Data were processed using MassLynx V4.2.

HepG2 cell culture and treatment

HepG2 cells were obtained from the American Type Culture Collection and cultured in Minimum Essential Medium (Cytiva, AJ30742834) containing 10% fetal bovine serum (Gibco), 1% non-essential amino acids (Gibco, 11140050) and 1% penicillin – streptomycin (MeilunBio, MA0110) at 37 ° C in 5% CO 2. Lipid accumulation was induced using 500 μM sodium palmitate and 250 μM sodium oleate (Kunchuang Biotechnology, KC006) for 48 h. Cells were treated with 50 μM acetylcarnitine for 24 h.

Cell viability assay

Cell viability was assessed using the Cell Counting Kit-8 (CCK-8) assay (MCE, NJ, USA, #HY-K0301) according to the manufacturer's protocol. Cells in 96-well plates were cultured approximately 90% confluence and treated with acetylcarnitine for 24 h, followed by adding 10 μL of CCK-8 reagent into each well and incubated for another 3 h. The absorbance of the formazan product was measured at 450 nm using a Spark 10 M (Tecan Austria GmbH Untersbergstr, Grödig, Austria), with appropriate

blank controls included in each assay.

Filipin staining

HepG2 cells cultured on the glass coverslips were fixed with 4% paraformaldehyde followed by washing twice with PBS and incubated with 50 μg/mL filipin III (GlpBio, Montclair, CA, USA, #GC12048) in PBS for 1 h at room temperature in dark. After three times washes with PBS, DAPI was added in and pictures were taken using the Zeiss Axio Observer Fluorescence Microscope (LSM980).

Cellular cholesterol and triglyceride measurements

HepG2 cells in 12-well plate were treated as indicated followed by the total cholesterol and triglyceride measurement using the commercial kit (Applygen Technologies Inc., Beijing, China) according to the manufacturer's instructions.

Plasmids and siRNAs

The human CYP7A1 coding sequence was cloned into pcDNA3.1. Two siRNAs targeting human CYP7A1 were synthesized by AuGCT; sequences are listed in Supplementary Table 2. Knockdown was assessed in HepG2 and 293T cells, and siCYP7A1-2 was selected for the functional experiments.

Statistical analysis

Data are presented as the mean ± standard error of the mean (SEM). Statistical analyses were performed using SPSS (version 18.0; SPSS Inc., Chicago, IL, USA), with the appropriate statistical tests selected based on the experimental design: two-tailed Student's t-test for comparisons between two groups or one-way analysis of variance (ANOVA) for multiple group comparisons. Statistical significance was set at $*p < 0.05$, with specific thresholds denoted as $**p < 0.01$ and $***p < 0.001$. "NS" indicates non-significance. Data visualization and graphical representations were generated using GraphPad Prism 9.0 (GraphPad Software Inc., San Diego, CA, USA) and R statistical software (version 4.4.2). Schematic illustrations of the animal experimental designs were created using BioRender (https://biorender.com).

Data availability

The metabolomics data have been deposited to MetaboLights under accession

MTBLS12961, https://www.ebi.ac.uk/metabolights/reviewer69b0322a-5345-4a59-9253-86d759496bd1. Additional data supporting the findings are available in the article and its Supplementary Information or from the corresponding author on reasonable request.

Author contributions

Y.-M.Z.: Investigation, Methodology, Data curation, Writing-original draft, Funding acquisition. L.C.: Methodology, Validation, Writing-review & editing. X.-X.L.: Investigation, Methodology, Data curation. L.Z.: Investigation, Methodology. H.-S.H.: Investigation. C.-X.C.: Formal analysis, Visualization. L.-Y.J.: Methodology, Investigation. H.-Y.M.: Investigation, Methodology. K.H.: Methodology, Conceptualization. Y.Z.: Investigation, Methodology. X.-M.S.: Visualization, Resources. X.-K.L.: Validation, Writing- review & editing. Q.Z.: Methodology, Investigation. Z.-C.M.: Validation, Resources. Z.Z.: Validation, Resources. M.-L.J.: Supervision, Conceptualization, Writing-review & editing, Funding acquisition.

Competing Interests

The authors declare no competing financial or non-financial interests.

Acknowledgements

This study was supported by the National Natural Science Foundation of China (32302853), the Hubei Provincial Agricultural Key Core Technology Tackling Project (HBNYHXGG2023-3), and the Open Project of Hubei Jiangxia Laboratory (2025JXKF006).

References

1. NCD Risk Factor Collaboration (NCD-RisC). Repositioning of the global epicentre of non-optimal cholesterol. *Nature* **582**, 73–77 (2020).
2. Grundy, S. M. et al. 2018 AHA/ ACC/ AACVPR/ AAPA/ ABC/ ACPM/ADA/ AGS/APhA/ ASPC/ NLA/PCNA guideline on the management of blood cholesterol: a report of the American College of Cardiology/American Heart Association Task Force on Clinical Practice Guidelines. *Circulation* **139**, e1082–e1143 (2019).
3. Stroes, E. S. et al. Statin-associated muscle symptoms: impact on statin therapy—European Atherosclerosis Society Consensus Panel Statement on Assessment, Aetiology and Management. *Eur. Heart J.* **36**, 1012–1022 (2015).
4. Mach, F. et al. 2019 ESC/EAS Guidelines for the management of dyslipidaemias: lipid modification to reduce cardiovascular risk. *Eur. Heart J.* **41**, 111–188 (2020).
5. Luo, J., Yang, H. & Song, B. L. Mechanisms and regulation of cholesterol homeostasis. *Nat. Rev. Mol. Cell Biol.* **21**, 225–245 (2020).
6. Xu, Y. et al. Farnesoid X receptor activation increases reverse cholesterol transport by modulating bile acid composition and cholesterol absorption in mice. *Hepatology* **64**, 1072–1085 (2016).
7. Li, T. & Chiang, J. Y. L. Bile acid signaling in metabolic disease and drug therapy. *Pharmacol. Rev.* **66**, 948–983 (2014).
8. Pullinger, C. R. et al. Human cholesterol 7α-hydroxylase (CYP7A1) deficiency has a hypercholesterolemic phenotype. *J. Clin. Invest.* **110**, 109–117 (2002).
9. Li, T. et al. Transgenic expression of cholesterol 7α-hydroxylase in the liver prevents high-fat diet-induced obesity and insulin resistance in mice. *Hepatology* **52**, 678–690 (2010).
10. Zhang, Z. C., Zhou, Q., Huangfu, G. Y., Wu, Y. & Zhang, J. L. Anthocyanin extracts of lingonberry (*Vaccinium vitis-idaea* L.) attenuate serum lipids and cholesterol metabolism in HCD-induced hypercholesterolaemic male mice. *Int. J. Food Sci. Technol.* **54**, 1576–1587 (2019).
11. Jiang, H. et al. An advance on nutritional profile, phytochemical profile, nutraceutical properties, and potential industrial applications of lemon peels: a comprehensive review. *Trends Food Sci. Technol.* **124**, 219–236 (2022).
12. Gil-Izquierdo, A., Riquelme, M. T., Porras, I. & Ferreres, F. Effect of the rootstock and interstock grafted in lemon tree (*Citrus limon* (L.) Burm.) on the flavonoid content of lemon juice. *J. Agric. Food Chem.* **52**, 324–331 (2004).
13. Caristi, C. et al. Flavonoids detection by HPLC-DAD-MS-MS in lemon juices from Sicilian cultivars. *J. Agric. Food Chem.* **51**, 3528–3534 (2003).
14. Fukuchi, Y. et al. Lemon polyphenols suppress diet-induced obesity by up-regulation of mRNA levels of the enzymes involved in β-oxidation in mouse white adipose tissue. *J. Clin. Biochem. Nutr.* **43**, 201–209 (2008).
15. Pan, Y. et al. Anti-obesity effect of fermented lemon peel on high-fat diet-induced obese mice by modulating the inflammatory response. *J. Food Biochem.* **46**, e14200 (2022).
16. Alasalvar, H., Kaya, M., Berktas, S., Basyigit, B. & Cam, M. Pressurised hot water extraction of phenolic compounds with a focus on eriocitrin and hesperidin from lemon peel. *Int. J. Food Sci. Technol.* **58**, 2060–2066 (2023).
17. Li, L. et al. A comprehensive study of eriocitrin metabolism in vivo and in vitro based on an efficient UHPLC-Q-TOF-MS/MS strategy. *RSC Adv.* **9**, 24963–24980 (2019).

18. Chen, L., Li, M., Wu, J. L., Li, J. X. & Ma, Z. C. Effect of lemon water-soluble extract on hyperuricemia in a mouse model. *Food Funct.* **10**, 6000–6008 (2019).
19. Wu, C. C. et al. Lemon fermented products prevent obesity in high-fat diet-fed rats by modulating lipid metabolism and gut microbiota. *J. Food Sci. Technol.* **60**, 1036–1044 (2023).
20. de Carvalho, I. O. A. M. et al. The use of lemon juice and its role in polyunsaturated fatty acid and cholesterol oxide formation in thermally prepared sardines. *J. Food Compos. Anal.* **104**, 104087 (2021).
21. Assini, J. M. et al. Naringenin prevents cholesterol-induced systemic inflammation, metabolic dysregulation, and atherosclerosis in *Ldlr*−/− mice. *J. Lipid Res.* **54**, 711–724 (2013).
22. Hiramitsu, M. et al. Eriocitrin ameliorates diet-induced hepatic steatosis with activation of mitochondrial biogenesis. *Sci. Rep.* **4**, 3708 (2014).
23. Sun, Y. Z., Chen, J. F., Shen, L. M., Zhou, J. & Wang, C. F. Anti-atherosclerotic effect of hesperidin in *Ldlr*−/− mice and its possible mechanism. *Eur. J. Pharmacol.* **815**, 109–117 (2017).
24. Sugasawa, N. et al. Inhibition of atherosclerotic plaque development by oral administration of α-glucosyl hesperidin and water-dispersible hesperetin in apolipoprotein E knockout mice. *J. Am. Coll. Nutr.* **38**, 15–22 (2019).
25. Rosca, M. G., Lemieux, H. & Hoppel, C. L. Mitochondria in the elderly: is acetylcarnitine a rejuvenator? *Adv. Drug Deliv. Rev.* **61**, 1332–1342 (2009).
26. Lu, Y. et al. Acetylcarnitine is a candidate diagnostic and prognostic biomarker of hepatocellular carcinoma. *Cancer Res.* **76**, 2912–2920 (2016).
27. Izzo, L. T. et al. Acetylcarnitine shuttling links mitochondrial metabolism to histone acetylation and lipogenesis. *Sci. Adv.* **9**, eadf0115 (2023).
28. Wahlström, A., Sayin, S. I., Marschall, H. U. & Bäckhed, F. Intestinal crosstalk between bile acids and microbiota and its impact on host metabolism. *Cell Metab.* **24**, 41–50 (2016).
29. Rizzolo, D. et al. Bile acid homeostasis in a cholesterol 7α-hydroxylase and sterol 27-hydroxylase double knockout mouse model. *Hepatology* **70**, 389–402 (2019).
30. Rizzolo, D. et al. Bile acid homeostasis in female mice deficient in *Cyp7a1* and *Cyp27a1*. *Acta Pharm. Sin. B* **11**, 3847–3856 (2021).
31. Donia, M. S. & Fischbach, M. A. Human microbiota: small molecules from the human microbiota. *Science* **349**, 1254766 (2015).

Figures

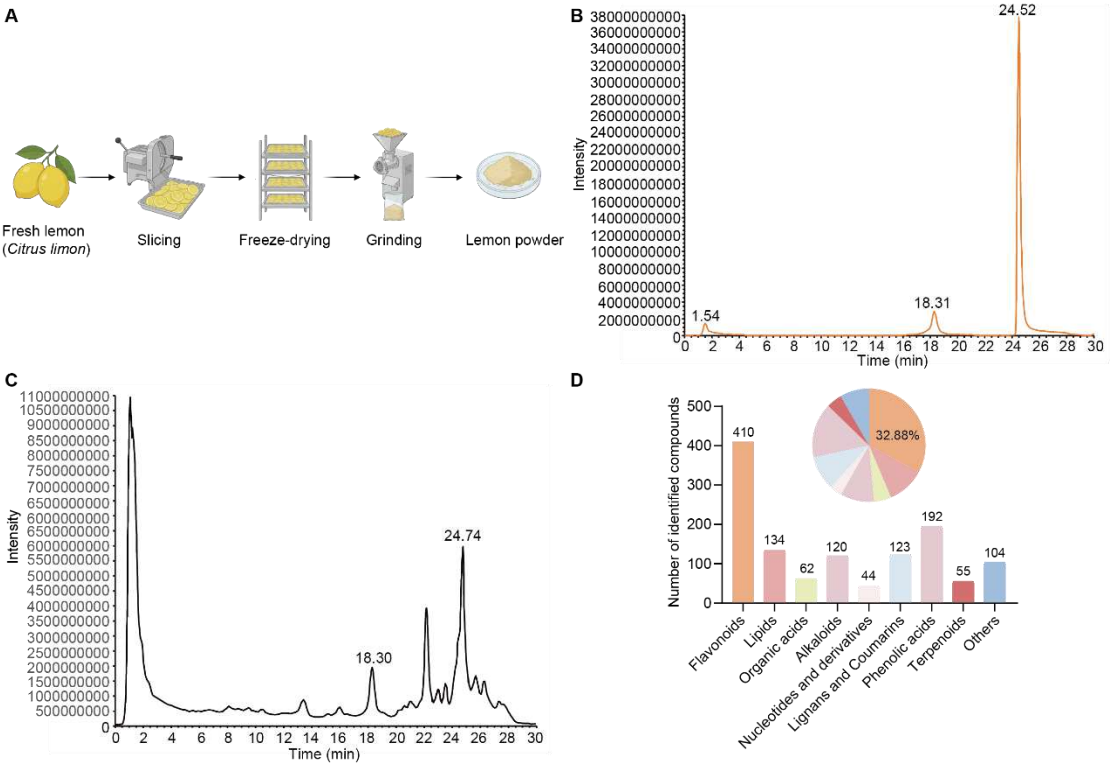


Figure 1. Preparation and chemical characterization of lemon powder.

(A) Preparation of lemon powder. (B) Chemical fingerprint profiling of lemon powder. (C) Identification of representative compounds. (D) Chemical composition profiling of lemon powder.

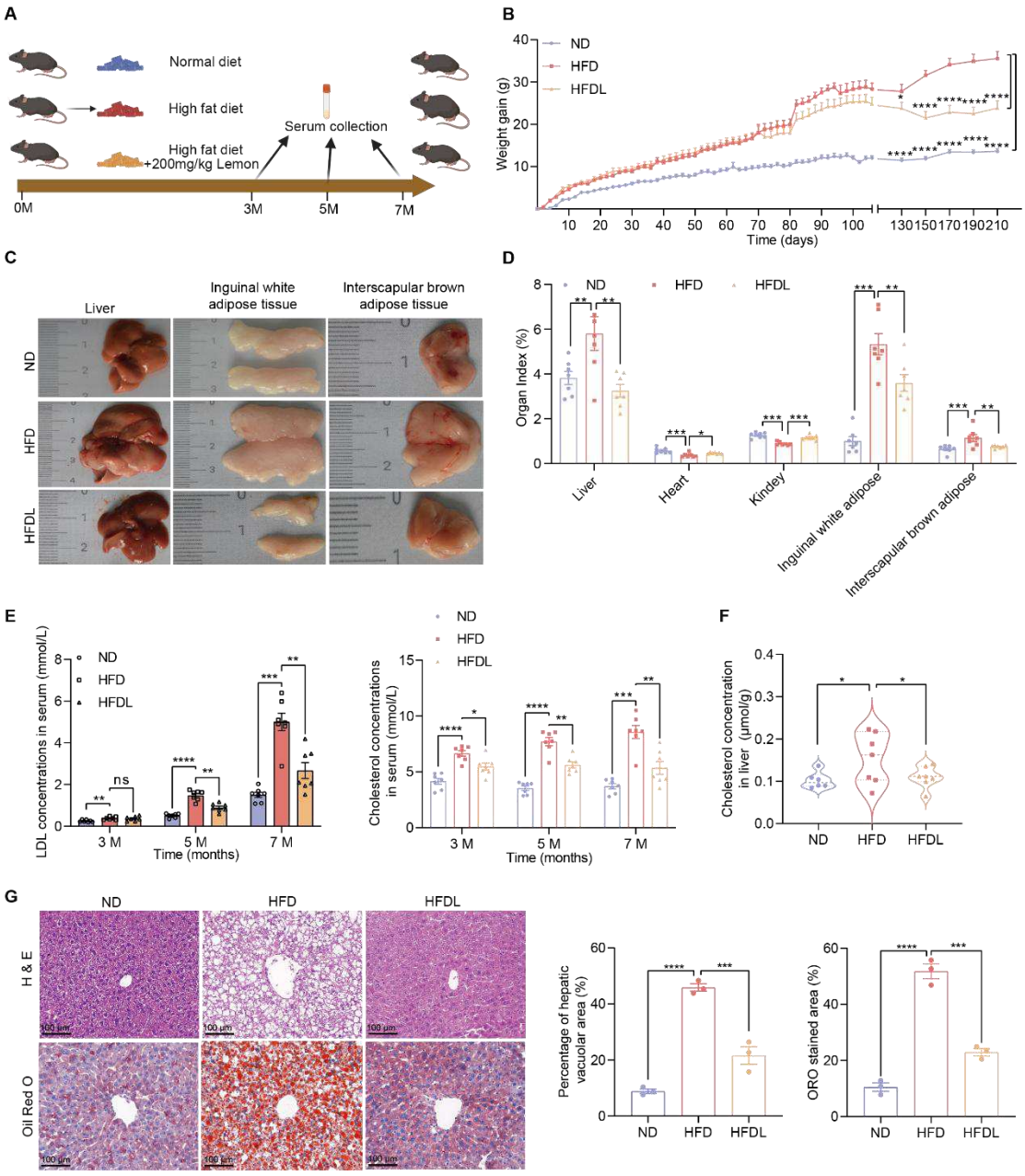


Figure 2. Lemon supplementation alleviates diet-induced hypercholesterolemia.

(A) Experimental design: 8-week-old male C57BL/6J mice were fed a normal diet (ND), high-fat diet (HFD), or HFD supplemented with 200 mg/kg lemon (HFDL) for 7 months. Serum was collected at three, five and seven months (n=12/group). (B) Body weight trajectory (n=12/group). (C) Gross morphology of liver, inguinal white adipose tissue, and interscapular brown adipose tissue. (D) Organ-to-body weight ratios of liver, heart, kidney, inguinal white adipose tissue, and interscapular brown adipose tissue (n=7/group). (E) Serum low-density lipoprotein cholesterol (LDL-C) and cholesterol levels at three, five and seven months (n=7/group). (F) Hepatic cholesterol

concentration (n=7/group). (G) H&E and ORO-staining of liver sections (scale bar=100 μm) (n=3/group). Data are expressed as mean ± SEM. *p<0.05, **p<0.01, ***p<0.001 by one-way ANOVA with Tukey's post hoc test. Body weight changes were analyzed using two-way mixed-design ANOVA with repeated measures over time.

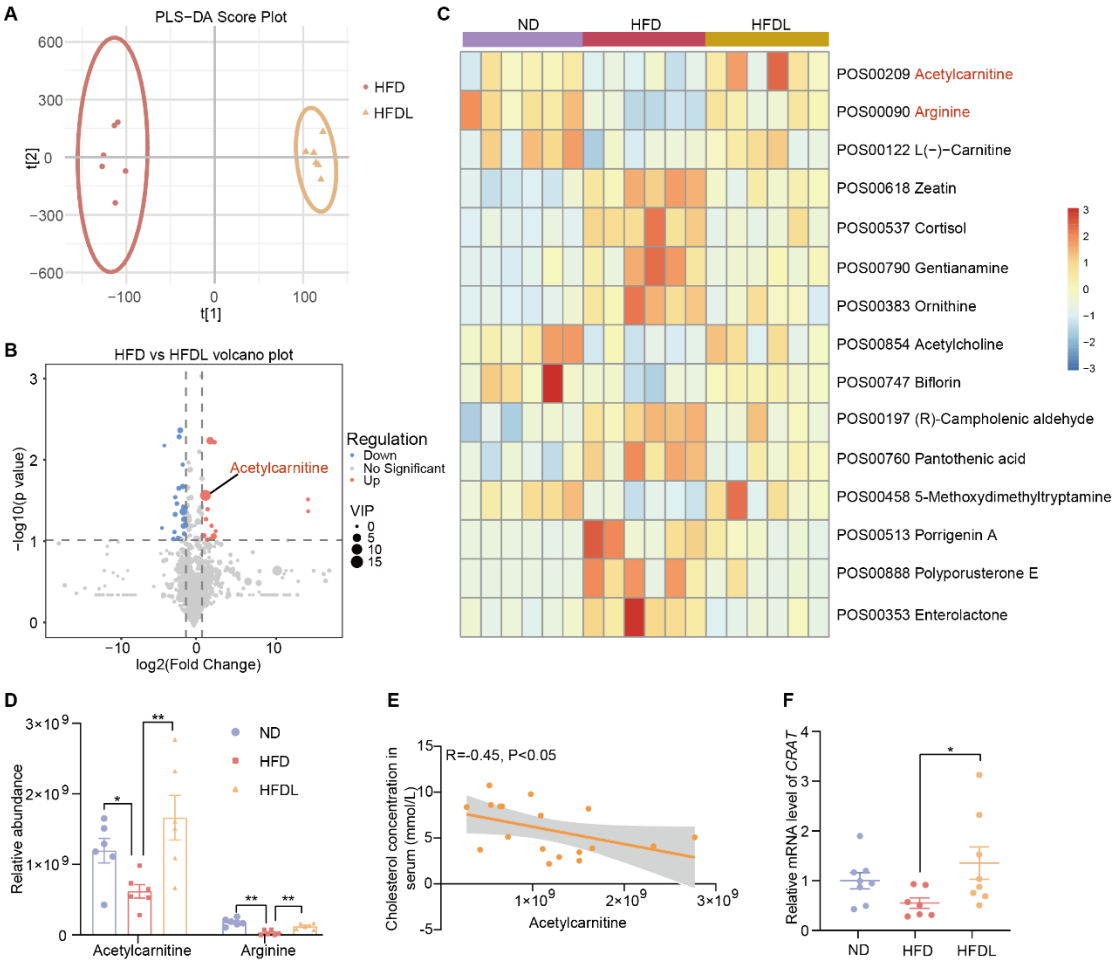


Figure 3. Lemon supplementation reshapes host metabolism and elevates acetylcarnitine levels.

(A) PLS-DA showing differences in metabolite composition between the HFD and HFDL groups (n=6/group). (B) Volcano plot comparison of HFD vs HFDL. Each point in the volcano plot represents a metabolite, the abscissa represents the fold change of each substance in the group compared to each other (log 2), and the ordinate represents the P-value of the student's t-test (taking the pair with base 10). The size of the scatter point corresponds with the VIP value. Significantly upregulated and downregulated metabolites are presented in red and blue, respectively (n=6/group). (C) Hierarchical clustering analysis in positive ion mode. The abscissa represents different experimental groups, the ordinate represents the differential metabolites compared in the group, the color blocks represent the relative expression levels of the metabolites at the corresponding positions, red indicates high expression levels, and blue indicates low expression levels. (D) Relative abundance of acetylcarnitine and arginine in ND, HFD

and HFDL group (n=6/group). (E) Correlation analysis between serum cholesterol and acetylcarnitine level (n=6/group). (F) Hepatic mRNA expression of carnitine acetyltransferase (*CRAT*) in ND, HFD, and HFDL group (n=8/group). Data are expressed as mean ± SEM. *p<0.05, **p<0.01 by one-way ANOVA with Tukey's post hoc test for multiple group comparisons, and two-tailed Student's t-test for comparisons between two groups.

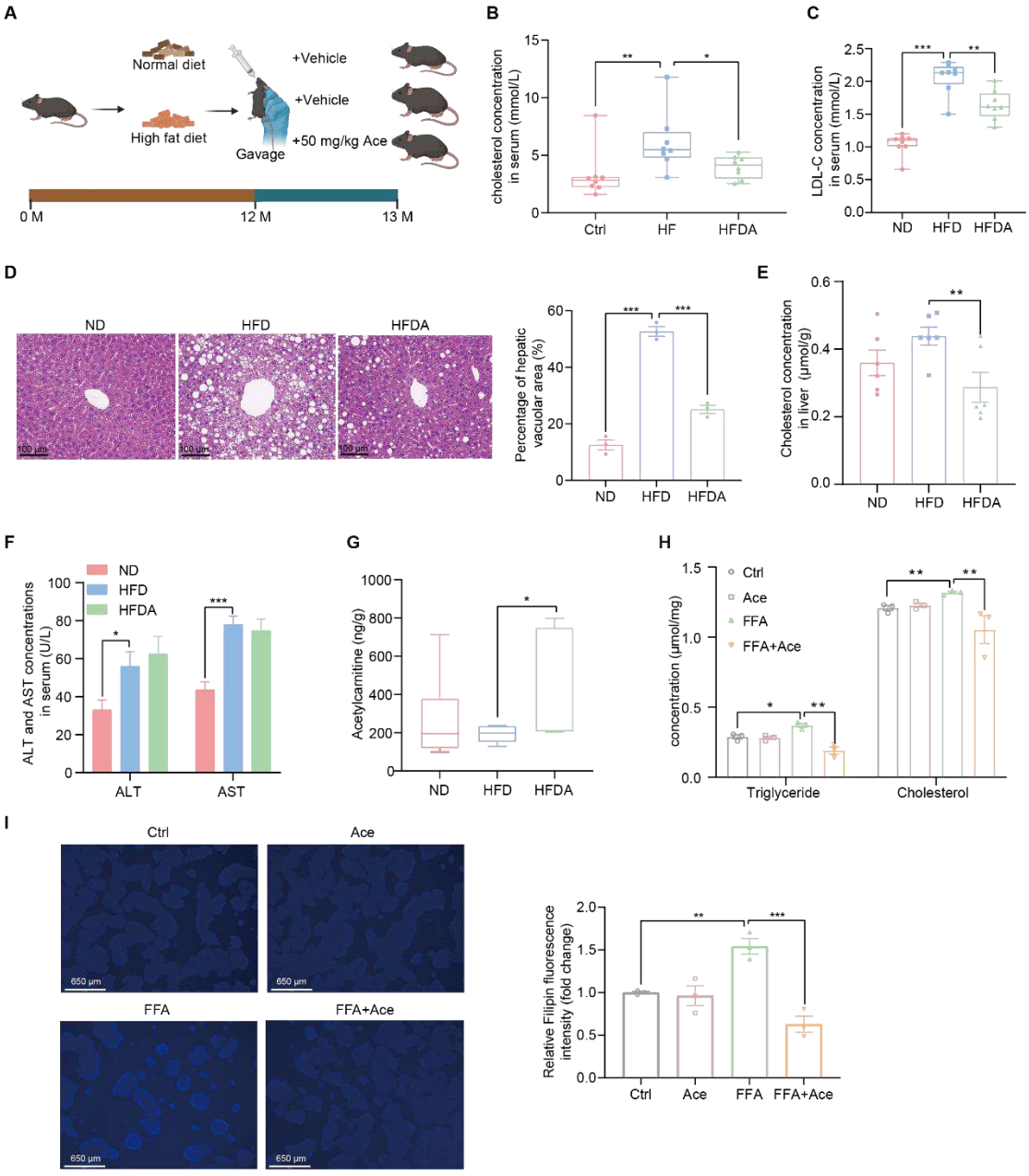


Figure 4. Acetylcarnitine alleviates hypercholesterolemia *in vivo* and *in vitro*.

(A) Experimental design: 8-week-old male C57BL/6J mice were fed a normal diet (ND) and high-fat diet (HFD) for 12 months, and then ND mice oral gavage with PBS, HFD mice oral gavage with PBS and 50 mg/kg of acetylcarnitine (HFDA) for one month (n=8/group). (B, C) Serum cholesterol and LDL-C levels (n=8/group). (D) Serum alanine aminotransferase (ALT) and aspartate aminotransferase (AST) levels (n=6/group). (E) Liver H&E staining (scale bar =100 μm) (n=3/group). (E) Hepatic cholesterol concentration (n=6/group). (G) Hepatic acetylcarnitine concentration (n=6/group). (H) Representative images of Filipin staining in HepG2 cells (n=3/group).

(I) Triglyceride and cholesterol levels in HpeG2 cell (n=3/group). Data are presented as mean ± SEM. *p<0.05, **p<0.01, ***p<0.001 by one-way ANOVA with Tukey's post hoc test.

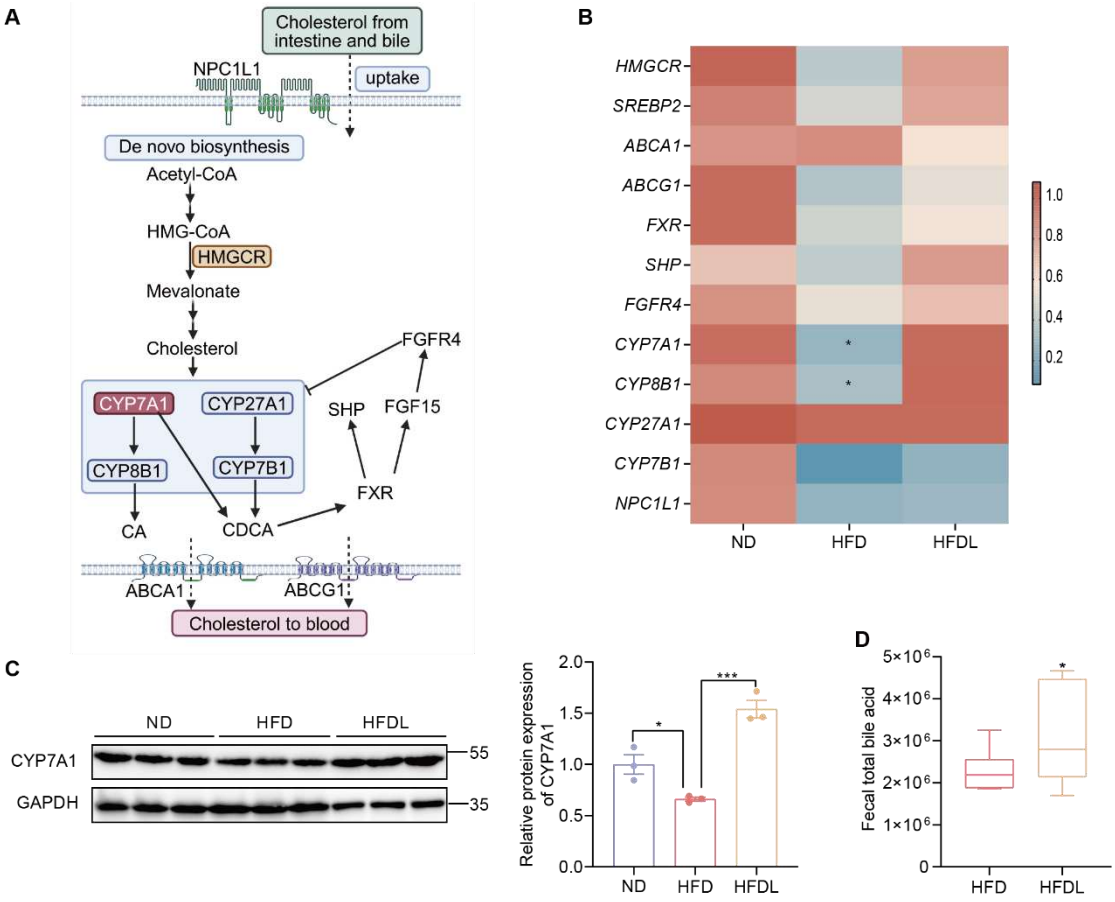


Figure 5. Lemon increases CYP7A1 and fecal bile acid levels.

(A) The diagram of cholesterol metabolic pathway. (B) Detection of the expression levels of cholesterol and bile acid metabolism-related genes by qPCR in liver (n=8/group). (C) Detection of hepatic CYP7A1 expression treated with lemon by western bolting (n=3/group). (D) Fecal total bile acid (n=7/group). Statistic analyze was performed by one-way ANOVA with Tukey's post hoc test for multiple group comparisons, and two-tailed Student's t-test for comparisons between two groups (*p<0.05, **p<0.01, ***p<0.001).

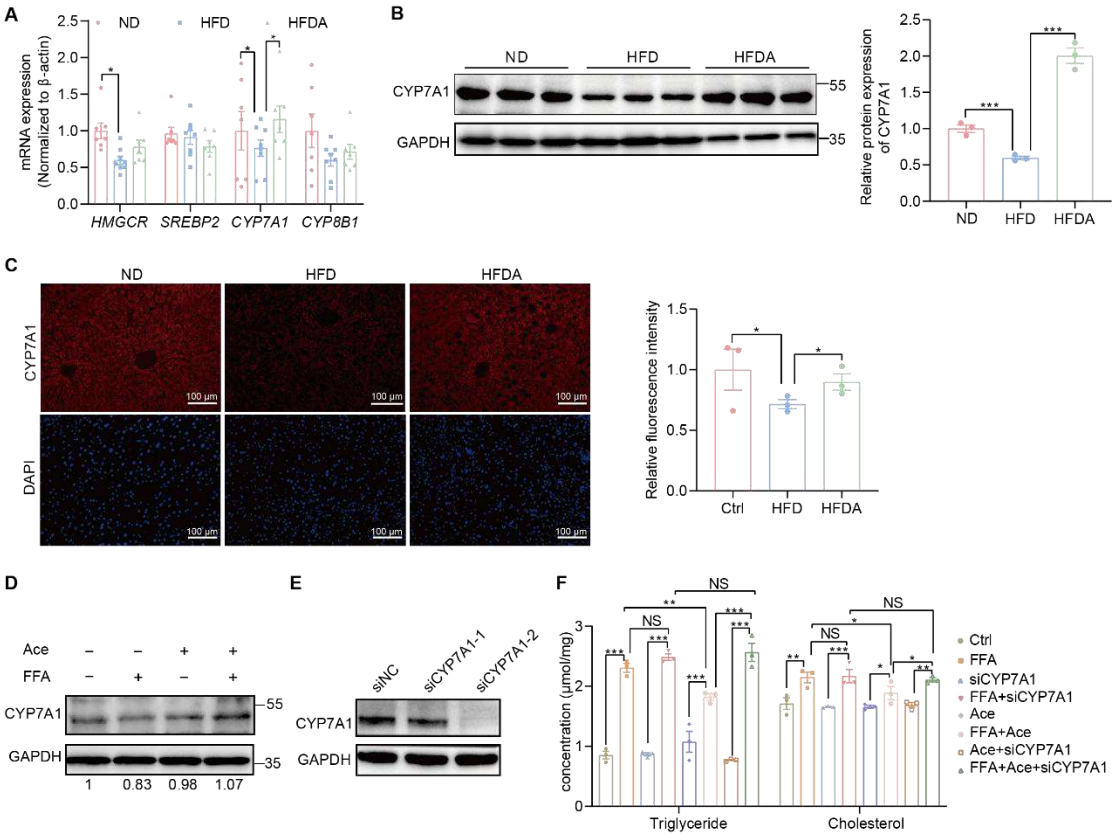


Figure 6. CYP7A1 contributes to the cholesterol-lowering response to acetylcarnitine.

(A) Detection of the expression levels of cholesterol and bile acid metabolism-related genes by qPCR in liver (n=7/group). (B) Detection of hepatic CYP7A1 protein expression in mice treated with acetylcarnitine by western bolting (n=3/group). (C) Hepatic immunofluorescence staining in mice treated with acetylcarnitine (n=3/group). (D) CYP7A1 expression in HepG2 cells treated with acetylcarnitine. (E) CYP7A1-specific siRNAs in HepG2 cells. (F) Triglyceride and cholesterol levels in HepG2 cells treated with FFA, Ace, or CYP7A1 siRNA. Data are presented as mean ± SEM. Statistic analyze was performed by one-way ANOVA with Tukey's post hoc test (*p<0.05, **p<0.01, ***p<0.001).

Supplementary information

Supplementary Figure 1. Short-term lemon powder dose screening. (A) Experimental design: 8-week-old male C57BL/6J mice were fed a normal chow diet (Ctrl), and a normal chow diet supplemented with 50 mg/kg, 100 mg/kg, 200 mg/kg, and 400 mg/kg lemon powder diet for 28 days (n=5/group). (B) Body weight curve (n=5/group). (C) Average daily food intake (n=5/group). (D) Serum triglyceride, cholesterol, HDL-C, and LDL-C concentrations at 28th day (n=5/group). (E) Serum ALT and AST levels (n=5/group). (F) Hepatic mRNA expression of cholesterol and bile acid metabolism-related genes (n=5/group). Data are expressed as mean ± SEM. *p<0.05, **p<0.01, ***p<0.001 by one-way ANOVA with Tukey's post hoc test.

Supplementary Figure 2. Energy intake and water consumption during lemon powder supplementation. (A, B) Energy and water intake of ND, HFD, and HFDL groups. Data are expressed as mean ± SEM. *p<0.05, **p<0.01, ***p<0.001 by one-way ANOVA with Tukey's post hoc test. Blood glucose data were analyzed using a two-way repeated measures ANOVA.

Supplementary Figure 3. Acetylcarnitine attenuates cholesterol elevation during HFD feeding. (A) Experimental design: 8-week-old male C57BL/6J mice were fed a normal diet (ND), high-fat diet (HFD), and HFD oral gavage with 50 mg/kg acetylcarnitine (HFDA) for 2 months (n=6/group). (B) Serum concentration of cholesterol and LDL-C (n=6/group). (C) Serum concentration of ALT and AST (n=6/group). *p<0.05, **p<0.01, ***p<0.001 by one-way ANOVA with Tukey's post hoc test.

Supplementary Figure 4. Acetylcarnitine viability testing and CYP7A1 siRNA screening. (A) Cell viability under different concentrations of acetylcarnitine treatment. (B) CYP7A1-specific siRNAs in 293T cells.

Supplementary Figure 5. Lemon powder changes fecal bile acid profiles. (A) Fecal bile acid level between HFD and HFDL groups (n=6/group). Data are expressed as mean ± SEM. *p<0.05, **p<0.01, ***p<0.001 by two-tailed Student's t-test.

Supplementary Table 1. Primers used in this study

Supplementary Table 2. Small interfering RNAs

Supplementary Files

This is a list of supplementary files associated with this preprint. Click to download.

- SupplementaryInformation.docx
- supplementaryfileWeaternblot.docx